

Using a Subsidiary Pillar for Local Scour Mitigation at Bridge Piers

Hesham Fouli¹, Shazy Shabayek²

¹ Department of Civil Engineering, King Saud University, Riyadh, Saudi Arabia.

² Department of Irrigation and Hydraulics, Faculty of Engineering, Ain Shams University, Cairo, Egypt.

Corresponding Author: Shazy Shabayek

Abstract: This paper presents an experimental study on local scour at circular bridge piers. The main objective was to examine the effect of placing a circular subsidiary pillar upstream of a single circular pier on the local scour that occurs at the latter. 46 experiments, in 2 sets, were performed. In set A, experiments were performed with the pier alone to compare live bed scour and clear water scour, to investigate the effect of Froude number on the scour hole dimensions and to observe the temporal development of the scour hole under clear water scour condition in order to estimate the time of equilibrium of scour. In set B, the experiments were performed with the pillar placed upstream of the pier. Clear water scour conditions were established and $F_r=0.2$ was used. Three different diameters for the pillar and six different spacings between the pier and the pillar were used. The scour hole profile was measured in all the experiments. It was found that the subsidiary pillar was very effective in reducing the maximum scour depth by approximately 50%. The results showed that the maximum reduction for the scour depth could be achieved by using three different combinations of spacing and relative diameters.

Keywords: Bridge Piers, Local Scour, Mitigation, Subsidiary Pillar.

Date of Submission: 09-12-2017

Date of acceptance: 21-12-2017

I. Introduction

Local scour around bridge piers has been one of the most common causes of bridge failures [1]. Over a period of 30 years, 1000 of about 600,000 bridges in the United States have failed and 60% of those failures were due to scour [2]. Local scour is the erosion of sediment around the bridge piers and abutments. It occurs due to the flow constriction at the bridge that causes an increase in the local shear stress and creates vortices that remove the soil material surrounding the bridge pier or abutment. Depending upon whether the approach flow is carrying sediment or not, the pier scour is classified as: (i) clear-water scour; when the approaching flow does not carry sediment and (ii) live-bed scour; when the approaching flow carries sediment. Moreover, the evolution of the scour hole differs: in clear water scour, the scour depth increases slowly and tends to reach a stable solution; in live bed conditions, the scour depth increases rapidly and tends to fluctuate around an equilibrium value due to the interaction between erosion and deposition [3].

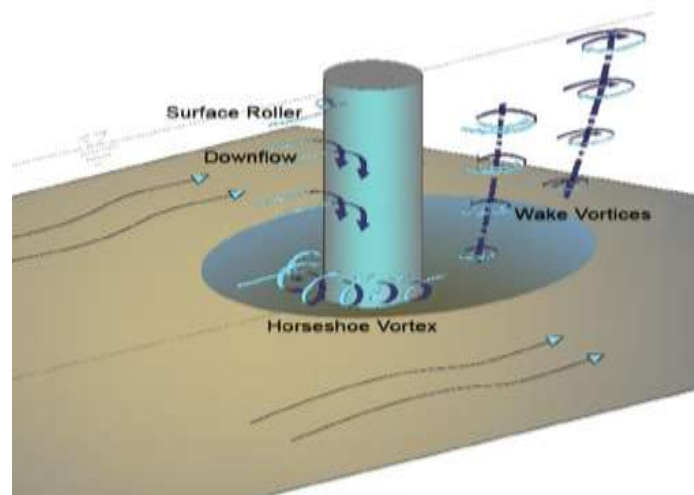


Fig. 1 Vortices and scour pattern around a cylindrical bridge pier. [4]

When unidirectional flow approaching the pier becomes three dimensional at the pier, a system of vortices start to form [5] and [6]. This system is composed of any or all of three basic types of vortices as shown in Fig. 1: (a) the horse shoe vortex at the base of the pier (b) the wake vortex downstream of the pier and (c) the surface roller ahead of the pier [7]. As the flow approaches the pier, a stagnation pressure gradient forms and causes a vertical component of a downward flow [8]. This downward flow acts as a jet and impinges on the bed eroding a groove adjacent to the front of the pier [6]. Due to the stagnation pressure, the water surface at the upstream of the pier rises and forms a surface roller [7]. The rolling up of unstable shear layers on the sides of the pier generates wake vortices and then the flow transports them downstream [9].

Scour countermeasures can be classified into two main categories: (a) bed armoring and (b) flow altering. In case of bed armoring, another layer of a more resistant material to shear stress, is added to protect the erodible material below. This layer includes: riprap stones, reno-mattresses, gabions, cable-tied blocks, concrete filled mats or bags and concrete aprons. Although riprap works well in most situations, [10] listed five failure mechanisms associated with its use at bridge piers namely: shear failure, winnowing failure, edge failure, bed-form induced failure and degradation failure. The flow altering devices act to reduce the strength of the vortex systems around the piers. These devices include: sacrificial piles/sills, collars, flow deflecting vanes, slots in the pier, suction applied to the pier [11].

In 2007, Haque et al. used sacrificial piles to mitigate scour around bridge piers [12]. The piles were arranged such that the scoured materials from the sacrificial pile filled the scour hole created upstream of the pier and was trapped inside it. They found that when the group of piles was placed at a distance of twice the projected width of the pier, the maximum scour depth was reduced by up to 50%.

In 2008, Chiew and Chen investigated experimentally the effect of suction on local scour around bridge piers under clear water conditions [13]. They concluded that for a suction flow rate of 2% of the total flow rate, the percentage reduction of the scour depth reached a maximum of 50% if the suction source was placed at less than 2.3 times of the pier diameter. Furthermore, the percentage reduction in the scour depth decreased for smaller suction flow rates.

In 2009, Hong Wu et al. investigated the use of frames in the shape of tetrahedrons as a pier-scour countermeasure [11]. The measurements of the velocity and turbulence intensity fields revealed that the frames created a deceleration region near the bed that was characterized by a significant reduction in the flow velocity, turbulence intensity and vorticity. This caused a reduction in the scour depth by 50%.

In 2013, Soltani et al. used jet injection through the pier body as a pier-scour countermeasure [14]. 1-Jet and 3-Jet injections were used at different jet locations and different angles between the jets under clear water conditions and two different flow depths. It was found that using the 3-Jet arrangement was not advantageous over the 1-Jet in the reduction of the scour depth for the shallower water depth. For the larger flow depth, the application of a jet with higher flow rate and more jet outlets when placed near the bed was more effective in reducing the scour depth.

In 2013, El-Ghorab conducted an experimental study based on reducing the flow stagnation and the vortices in front of the pier [15]. The pressure difference around the pier was used to drive the flow through arrangements of openings in the pier. Different opening diameters and different vertical spacings between the openings were used. The technique reduced the scour depth by up to 45%.

In 2016, Fouli and Elsebaie investigated the effect of placing triangular pillars with different apex angles of 60°, 90° and 120° upstream of single circular pier [16]. The triangular pillars were placed such that their apex faced the approach flow and their base length was equal to the pier diameter (D). Relative spacing (S/D) of 0, 0.5, 1, 1.5, 2 and 3 were tested. The highest reduction in the maximum scour depth (d_{sm}) of approximately 28% was obtained using S/D of 3 and an apex angle of 90° compared to the pier-alone case.

Some researchers combined two or more techniques for scour mitigation. In 2014, Akib et al. examined experimentally the use of collars and geobags, both separately and combined, to reduce the local scour at bridge piers [17]. The study proved that using a combination of steel collars and geobags resulted in the most significant reduction in scour. Furthermore, the study showed that using an independent steel collar was more efficient than using an independent geobag.

In 2009, Mashahir et al. used single and double collars to reduce scour around cylindrical bridge piers [18]. In combination with the single collar, bars were also installed at the downstream face of the pier to reduce the wake vortices. They found that the best arrangement that achieved 56% reduction in the scour depth and also decreased the scouring rate was when one collar was installed at the bed level and the second at one pier diameter below the bed. They also concluded that although the installation of bars did not reduce the maximum scour depth significantly, it postponed the start of the scouring at the upstream face of the pier.

The current study investigates experimentally a flow altering countermeasure against pier scour. The technique uses a single subsidiary pillar that is placed upstream of a circular bridge pier. Different pillar diameters and different spacings between the pier and the pillar were examined to assess the best configuration that gives maximum scour reduction at the pier.

II. Dimensional Analysis

The scour hole geometry at the pier depends on a multitude of variables including channel width, pier and pillar characteristics; i.e. ratio of their diameters and their inter-spacing, flow conditions; i.e. approach flow depth and discharge or velocity, sediment properties; mainly specific gravity and grain size, fluid kinematic and dynamic properties; i.e. density and viscosity, and time. Therefore for the depth of scour d_s , one can write:

$$d_s = f(W, D, D_s, S, y, V, g, d_{50}, \rho, \mu, t, t_o) \quad (1)$$

in which W is the width of channel, D is the diameter of bridge pier, D_s is the diameter of the subsidiary pillar, S is the clear internal spacing between the pillar and the pier, V is the velocity of flow, g is the gravitational acceleration, d_{50} is the median grain size, y is the approach flow depth, ρ is the density of fluid, μ is the viscosity of fluid, t_o is the time corresponding to the final scour hole depth and t is the time of scour hole depth development. Using the Pi theorem, it can be shown that:

$$\frac{d_s}{D} = f\left(\frac{W}{D}, \frac{y}{D}, \frac{D_s}{D}, \frac{S}{D}, F_r, \frac{d_{50}}{D}, R_e, \frac{t}{t_o}\right) \quad (2)$$

in which F_r is the approach flow Froude number, and R_e is its Reynolds number. After simplification of (2) and eliminating the variables that are not significantly relevant; i.e. R_e and those with constant values in this study; i.e. W , d_{50} , and y , (2) reduces to:

$$\frac{d_s}{D} = f\left(\frac{D_s}{D}, \frac{S}{D}, F_r, \frac{t}{t_o}\right) \quad (3)$$

Equation (3) will be used to describe the relationship between the scour hole depth as a function of the relevant variables in this study.

III. Experimental Setup and Experiments

The experiments were conducted in a rectangular flume 0.50m deep, 0.30m wide and 10.55m long as shown in Fig. 2. An energy dissipating plate is placed at the inlet to reduce the flow turbulence and prevent any floating parts from flowing into the flume. This, in addition to the length of the flume upstream of the testing section, resulted in having fully developed flow at the subsidiary pillar and the pier. The flume is constructed on an adjustable steel frame, with its bed approximately 1.60m above the laboratory floor. The flume is of the recirculating type where metal tanks, located under the flume, are used to collect the outflow and a pump is used to discharge it back into the flume. The pump has a capacity range of 70-180m³/hr. The flume is equipped with two control gates: one vertical sluice gate at the upstream inlet to the flume and a tailgate at the downstream end of the flume.

A layer of sand approximately 0.20m thick was placed in the working section. The size of the sand varied between 0.075mm and 2.000mm. Fig.3 shows the grain size distribution curve for the sand. The median sediment size was found to be 0.9mm. Sediment uniformity is defined by the uniformity factor σ_g where:

$$\sigma_g = \sqrt{\frac{d_{84}}{d_{16}}} \quad (4)$$

The sediment gradation curve Fig. 3 shows that the value of d_{84} is 1.04mm and that the value of d_{16} is 0.59. These values give a uniformity factor of 1.33. In 1991, Raudkivi suggested that soil material with $\sigma_g < 1.35$ is considered uniform [8]; therefore sediment non-uniformity will not affect the scour depth in this study.

A constant pier diameter of 0.03m was chosen throughout the experiments, making $D/W=0.1$, where D is the pier diameter and W is the flume width. The diameters of the subsidiary pillar, D_s , were chosen such that D_s/D was 2/3, 3/3, 4/3. In addition, six values for the spacing between the pier and the pillar, S , were used; $S=0, 0.5D, D, 1.5D, 2D$ and $3D$. Experiments were conducted for Froude numbers of 0.1, 0.2, and 0.3. The tailgate was used to maintain the depth of flow at 0.2m in all experiments.

A point-gauge mounted on a sliding aluminum frame was utilized to measure surface elevations. The discharge was measured by a V-notch installed at the downstream end according to the following equation:

$$Q = \frac{8}{15} C_d \tan \frac{\theta}{2} \sqrt{2g} (H - H_o)^{5/2} \quad (5)$$

Where Q is the discharge; C_d is the discharge coefficient and equals 0.6; g is the gravitational acceleration; $(H-H_o)$ is the head on the V-notch and θ is apex angle and equals 90 degrees.

Two sets of experiments, with 46 runs, were conducted. The primary details of these experiments are shown in Table 1. In Set A, which included experiments 1 to 28, only the pier was used. In Set B, which included experiments 29 to 46, the pier and the subsidiary pillar were used.

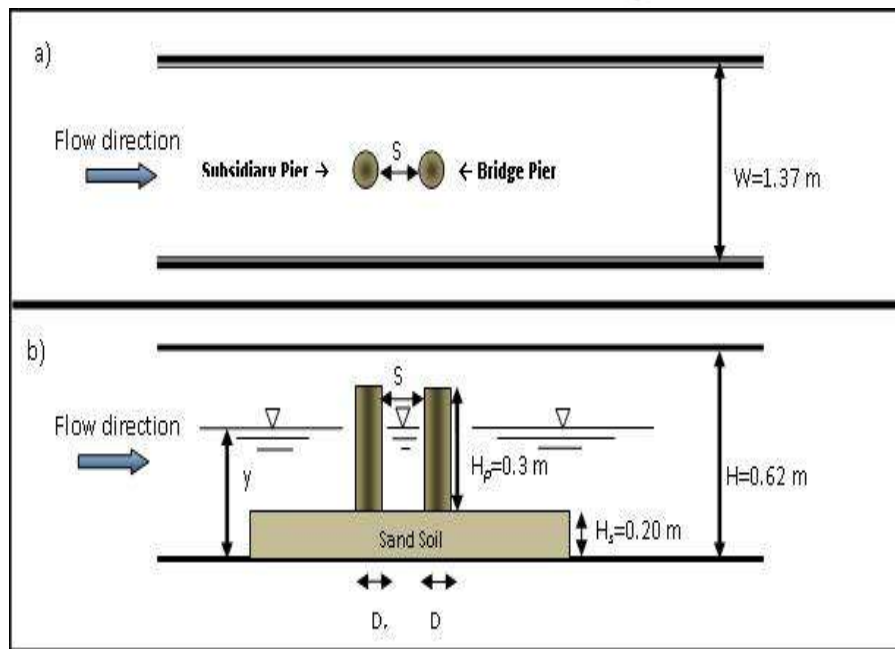
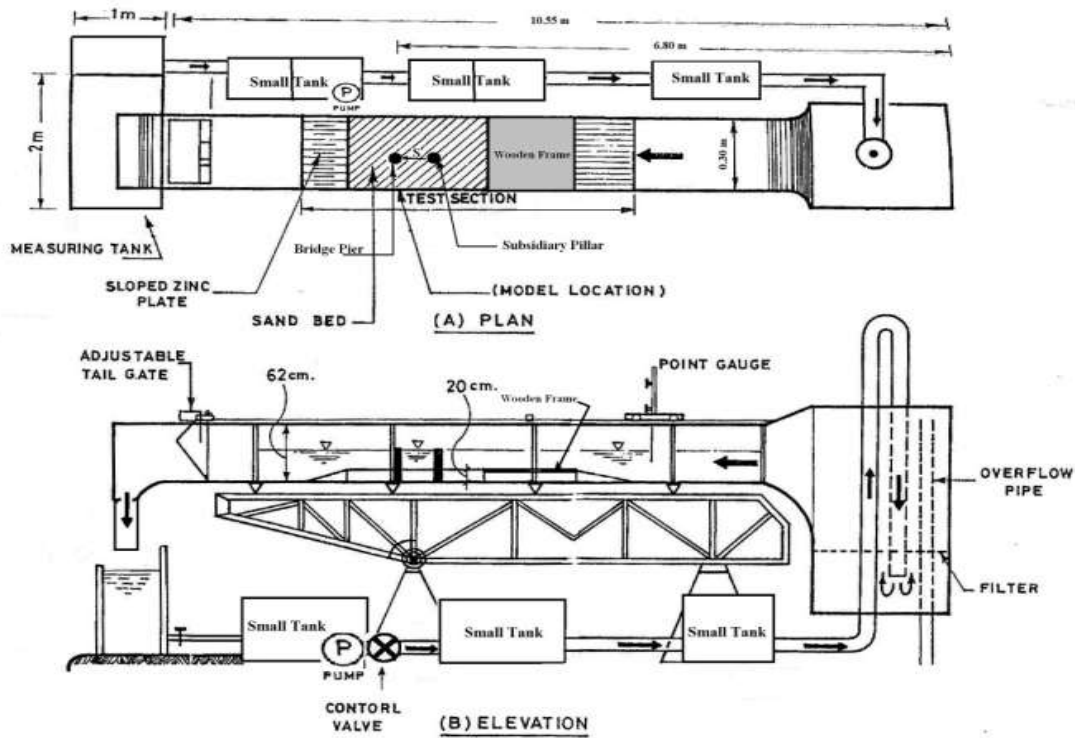


Fig. 2 Experimental setup: a) Plan view and b) Elevation (Front) view.
 (Detail A: Schematic definition of the test section) a) Plan view and b) Side view

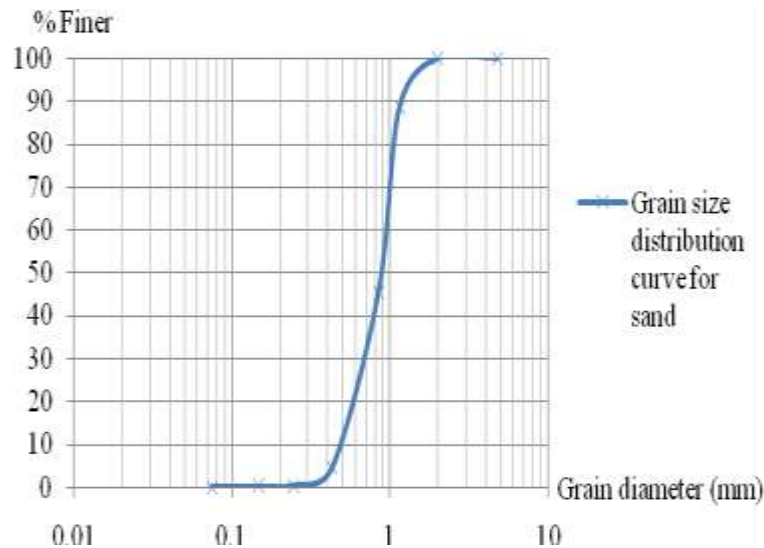


Fig. 3 Grain size distribution for the used sand

In Set A, experiments 1 to 7 and experiments 8 to 14 were conducted to compare live bed and clear water scour, in addition to estimating the time of equilibrium scour, t_0 . Experiments 8 to 28 were conducted to investigate the effect of Froude number on the scour hole dimensions and to observe the temporal development of the scour hole under clear water scour conditions. Experiments 1 to 28 were performed by allowing water to flow over the horizontal bed for different times (5, 15, 30, 60, 240, 360 and 720 minutes), to estimate the time to reach the equilibrium scour depth. In experiments 1 to 7, the pier was located at 6.20m from the start of the inlet channel and live bed scour occurred. In experiments 8 to 28, the pier was moved gradually upstream until no live bed scour was observed. The location of the pier for clear water scour in experiments 8 to 46 was 5.80m from the start of the inlet channel. As an additional precaution to avoid live bed scour, a wooden plate with fixed sand bed and glued gravel-sand mix was installed upstream of the test section as shown in Fig. 2.

In Set B, experiments 29 to 46 were performed to investigate the effect of the subsidiary pillar on the local scour at the pier. The experiments were repeated at increasing clear distance between the pier and the subsidiary pillar and with different diameters of the subsidiary pillar. The preliminary results obtained from experiments 1 to 28 were used as a guide in performing experiments 29 to 46. This refers to the time of equilibrium, t_0 , the location of the pier for clear water scour and the appropriate Froude number.

In Set B experiments, the pier and the subsidiary pillar were fixed on the flume bed approximately 5.80 m from the upstream gate. Sand was then placed and levelled in a wooden box with a depth of approximately 0.20 m. The sand was submerged with water and compacted before the experiments started and the sliding point-gauge was used to read the initial level of the sand bed before the flow started. The experiments were then started by allowing water to flow over the horizontal bed with a certain discharge. The depth, length and width of the scour hole in the sand bed were surveyed, using the point-gauge, when the equilibrium depth was reached. Before the beginning of a successive experiment, the sand bed was levelled to allow measuring the development of the new scour hole under the new flow and geometric conditions. The discharge was adjusted by using the control valve, tailgate and the head on the V-notch.

Table 1 Primary Details of Experiments

Set	Exp. Number	Scour Type	Froude Number	Time (min)	D_s (m)	S
A Pier only	1 – 7	Live Bed	0.1	t = 5, 15, 30, 60, 240, 360, 720	N/A	N/A
	8 – 14		0.1			
	15 – 21	Clear Water	0.2			
	22 – 28		0.3			
B Pier & Subsidiary Pillar	29 – 34	Clear Water	0.2	t = 360	0.02	S = 0, 0.5D, D, 1.5D, 2D, 3D
	35 – 40				0.03	
	41 – 46				0.04	

IV. Results and Analysis

4.1 Pier-alone Case

Fig. 4 presents the scour hole profiles for experiments 1 to 7 at different times (5, 15, 30, 60, 240, 360, and 720 minutes) for $F_r=0.1$ under live bed conditions. Fig. 4a shows the scour hole shape in the transverse direction while Fig. 4b shows the shape in the stream wise direction. The figure indicates a fluctuating cyclic pattern for the scour hole profile that is due to the erosion deposition behavior of the live bed scour in these experiments. The profiles in the Y-direction are symmetric about the pier's vertical axis and show a quasi-linear rate of decrease of d_s with Y that is almost the same for the different experiments. In the X-direction the scour hole profiles are asymmetrical about the pier's vertical axis. The profile has a steeper slope in the upstream than the downstream. The depth of scour is larger in the upstream than that at the downstream due to the stronger effect of the down-flow jet and the horse-shoe vortex than the wake vortices. The fluctuating cyclic pattern due to the live bed conditions is still noticeable.

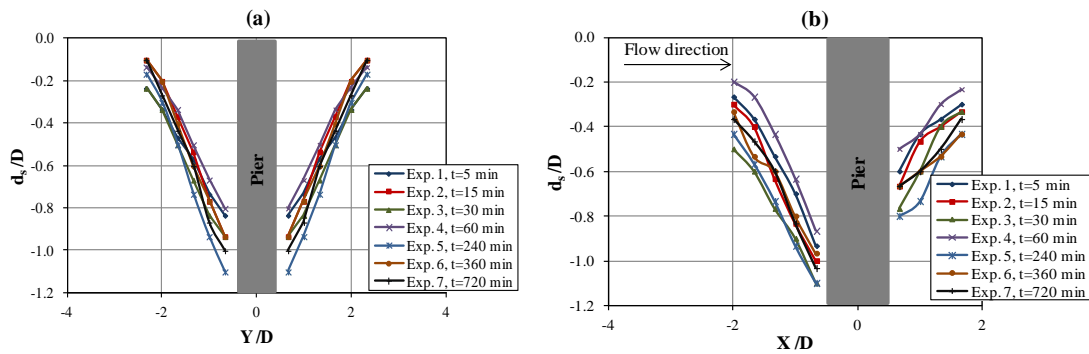


Fig. 4 Normalized scour hole profile (pier-alone case) at different times for $F_r=0.1$ under live bed conditions (a) transverse direction (b) stream wise direction

Fig. 5 presents the shape of the scour hole profiles for experiments 8 to 14 for $F_r=0.1$ under clear water conditions. In this case, a continuous increase in the scour depth with time, due to the erosion of the sand carried with the flow, is seen. The figure shows the same symmetrical profiles in the Y-direction and asymmetrical profiles in the X-direction as well as the increased effect of the horseshoe vortex in the upstream over the wake vortices in the downstream.

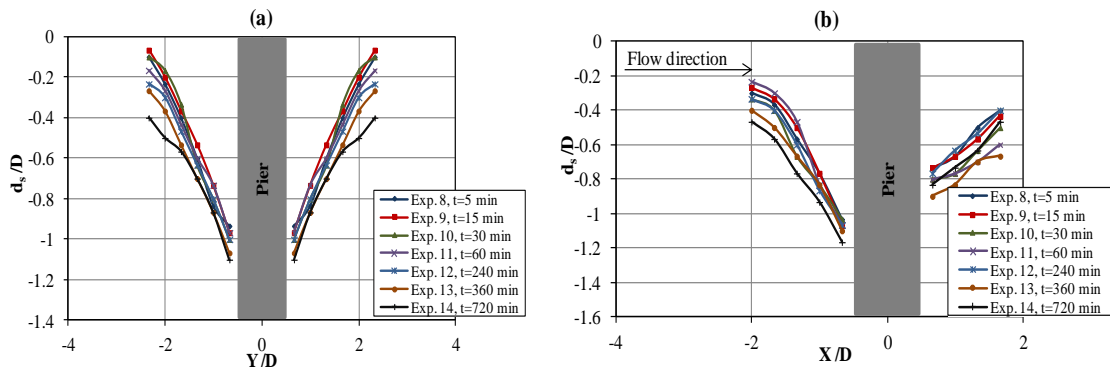


Fig. 5 Normalized scour hole profile (pier-alone case) at different times for $F_r=0.1$ under clear water conditions (a) transverse direction (b) stream wise direction

Fig. 6 presents the change in the normalized scour depth upstream of the pier ($X=-2$ cm) with the normalized time for experiments 1 to 7 (live bed scour) and 8 to 14 (clear water scour) at $F_r=0.1$. Based on the results of experiments 1 to 14, 94% of d_s occurs during 360 minutes therefore the maximum scour depth (d_{sm}) is measured at that time and the time of equilibrium, t_o , is considered to be 360 minutes in the following experiments. In Fig. 6, the depth of scour is normalized by the pier diameter, D , and the time is normalized by the time of equilibrium, t_o . The figure shows that in experiments 1 to 7, the scour depth fluctuates with time and three zones can be distinguished: Zone 1, where there is a rapid increase in the scour depth; Zone 2, where there is a cyclic fluctuating pattern, between deposition and erosion, in the d_s/D . The amplitude of these fluctuations decays gradually with time; Zone 3 where there is very slow erosion rate that results in a minimal increase in the d_s/D . In experiments 8 to 14, the figure shows a continuous increase in the scour depth with time which indicates an erosive behavior only for the clear water scour case.

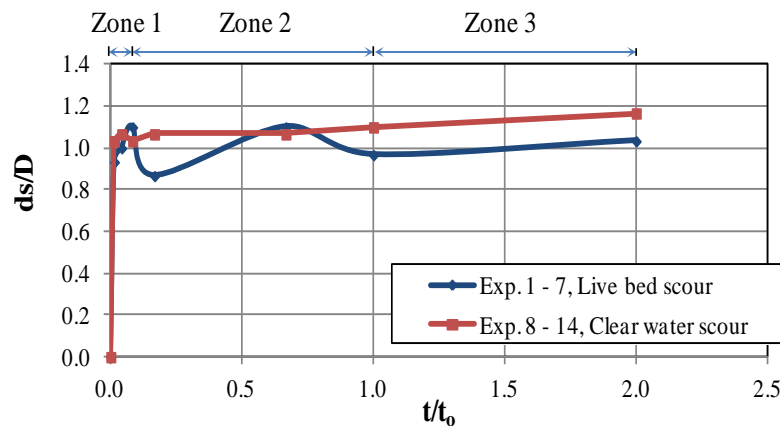


Fig. 6 Comparison between live bed and clear water scour depth near the pier for $F_r=0.1$

To investigate the effect of F_r on the clear water scour development, experiments 15 to 21 and experiments 22 to 28 were conducted for F_r equals to 0.2 and 0.3, respectively, for the different times (5, 15, 30, 60, 240, 360, and 720 minutes). The profiles in the Y-direction and the X-direction showed the same characteristics as those seen in Fig. 5a and 5b, respectively. Fig. 7a and 7b present the dimensions and the shape of the scour hole for different Froude numbers at the equilibrium time (t_0) in the transverse direction and in the stream wise direction, respectively. The figure shows that the quasi-linear decrease of d_s/D is almost the same for $F_r = 0.1$ and 0.2. However for $F_r = 0.3$ the rate of decrease of d_s/D decreases significantly starting from $Y = \pm 1.5$. Fig. 7b shows that the scour hole extended a long distance upstream of the pier for $F_r = 0.3$. In addition, underneath erosion below the wooden plate was observed during the experiments. Therefore, it was decided to use F_r of 0.2 in experiments 29 to 46, as it provided larger scour depths than $F_r = 0.1$ yet the scour hole profiles were within the flume's side boundaries and did not extend to the wooden plate.

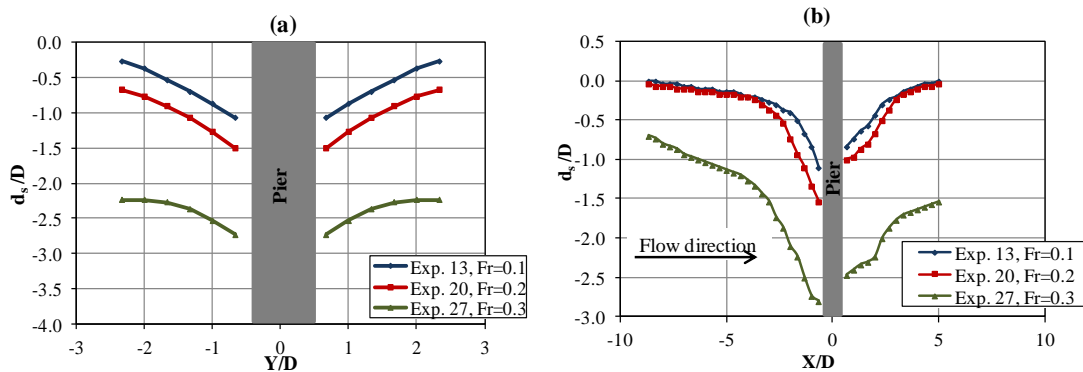


Fig. 7 Normalized scour hole profile for different Froude numbers at equilibrium time (Pier alone case); (a) transverse direction (b) stream wise direction

4.2 Pier-Pillar Case

Experiments 29 to 46 were conducted at $F_r = 0.2$, under clear water scour conditions, with the subsidiary pillar placed upstream of the pier at different spacing, S , of 0, 0.5D, D, 1.5D, 2D, 3D. Three diameters for the subsidiary pillar, D_s , were used such that $D_s/D=0.67, 1.00$, and 1.33. In all these experiments the scour hole profile was surveyed using the point gage after the water flowed for 360 minutes; this has been shown earlier to be the estimated equilibrium time for scour, t_0 (see Fig. 6).

Figs.8, 9, 10 show a sample of the stream wise X-direction profiles for $S=0, 1.5D$, and 3D, respectively. Fig.8 (a), (b), and (c) show the scour hole profile in the stream wise X-direction along the centerline of the pier and the pillar for experiments 29, 35, and 41 ($S=0$) for the different diameter ratios of 0.67, 1.00 and 1.33, respectively. Fig. 9 (a), (b), and (c) show the stream wise profile for experiments 32, 38, 44 ($S=1.5D$) for the three diameter ratios, respectively. Fig 10 (a), (b), and (c) show the stream wise profile for experiments 34, 40, and 46 for ($S=3D$) for the three diameter ratios, respectively. The profiles show that the upstream bed has a quasi linear slope up to a certain location beyond which it attains a milder slope and then it may flatten to

become almost horizontal or show signs of deposition. In the wake of the pier, the bed profile attains irregular patterns that may be non linear, leveled or quasi linear. In all the experiments 29 to 46, the scour depth near or right upstream of the pier is smaller than that upstream of the pillar. This illustrates the effect of the pillar in reducing the scour at the pier since it absorbs the initial shock of the approach flow.

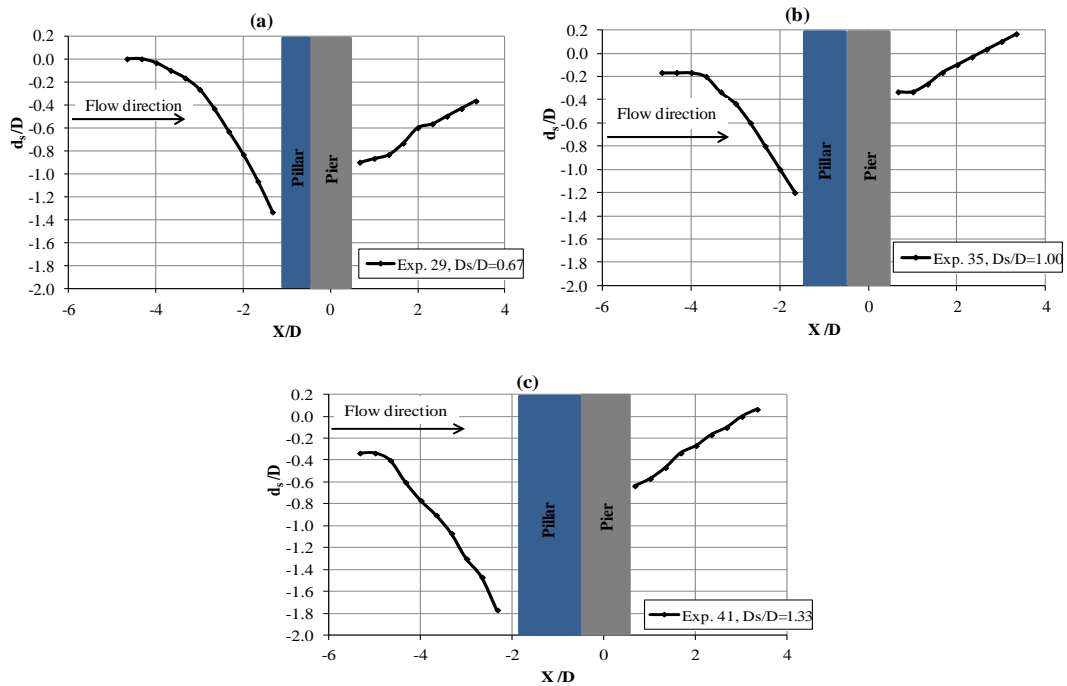


Fig. 8 Normalized scour hole longitudinal profile at $F_r=0.2$ for $S=0$ (a) $D_s/D=0.67$, (b) $D_s/D=1.00$, and (c) $D_s/D=1.33$

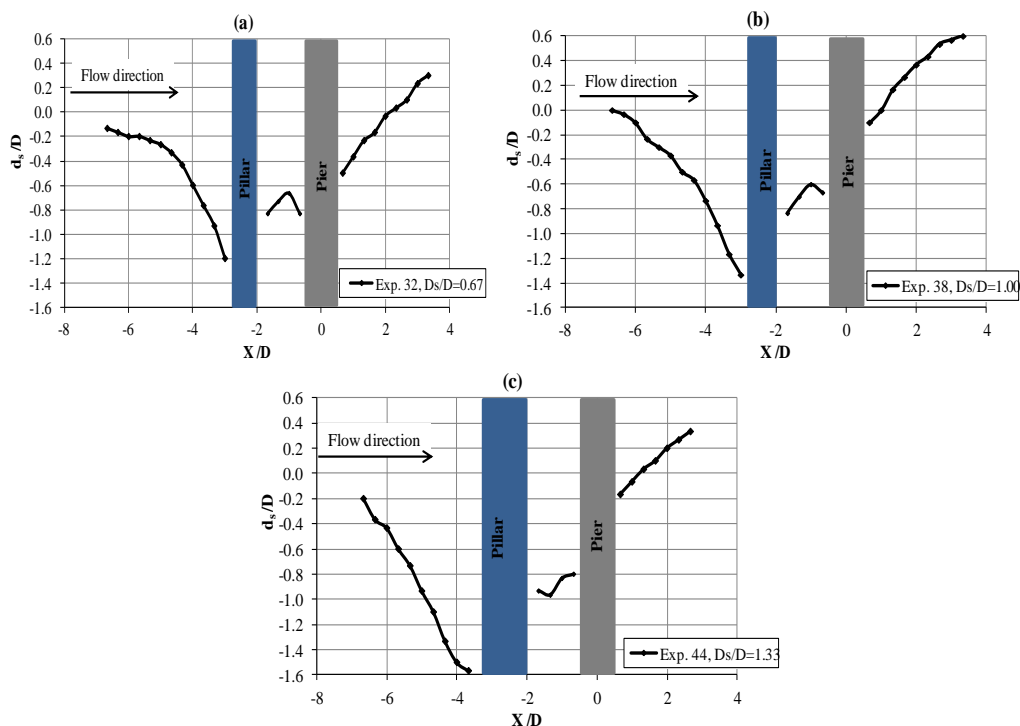


Fig. 9 Normalized scour hole longitudinal profile at $F_r=0.2$ for $S=1.5D$ (a) $D_s/D=0.67$, (b) $D_s/D=1.00$, and (c) $D_s/D=1.33$

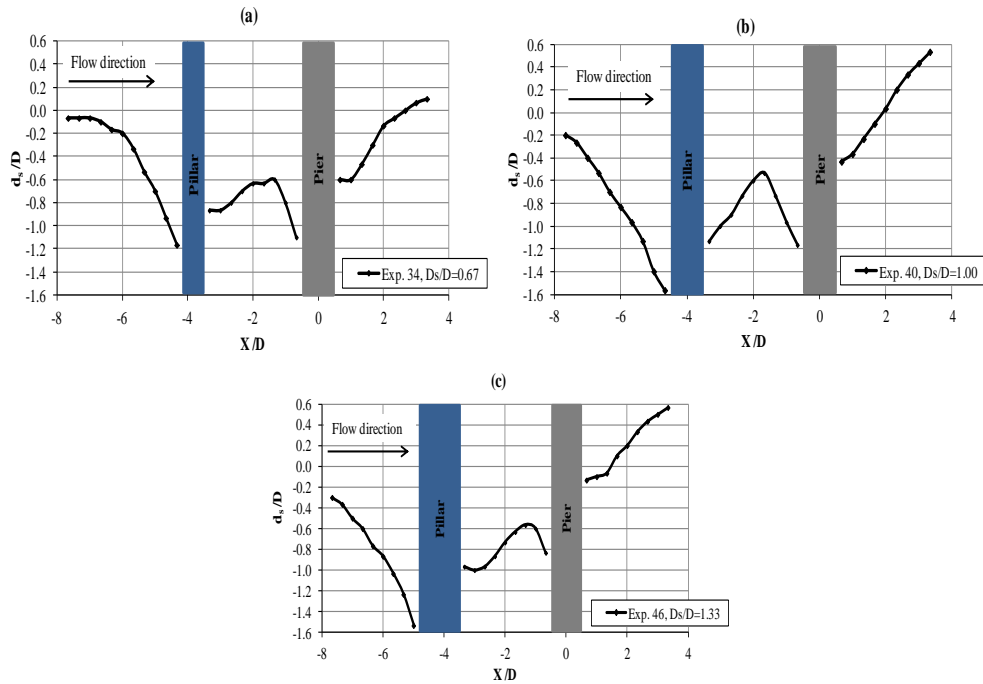


Fig. 10 Normalized scour hole longitudinal profile at $F_r=0.2$ for $S=3D$ (a) $D_s/D=0.67$, (b) $D_s/D=1.00$, and (c) $D_s/D=1.33$

Figs. 11 and 12 show the scour hole profiles in the transverse Y-direction across the centerline of the pier and the pillar, respectively. Fig. 11 (a), (b), and (c) present the profiles at the pier for experiments 29 to 34 ($D_s/D=0.67$), experiments 35 to 40 ($D_s/D=1.00$), and experiments 41 to 46 ($D_s/D=1.33$), respectively. The plots show that for each D_s/D value, the profiles fluctuate as S increases. These fluctuations are however least pronounced when $D_s/D=1.33$ (Fig.11(c)). Generally the profiles have a single quasilinear slope or may start with a steeper slope near the pier and end with a milder slope at the edge of the scour hole. Fig. 12 (a), (b), and (c) present the profiles at the pillar for experiments 29 to 34 ($D_s/D=0.67$), experiments 35 to 40 ($D_s/D=1.00$), and experiments 41 to 46 ($D_s/D=1.33$), respectively. The plots demonstrate that, similar to those of the pier, the profiles at the pillar fluctuate for each D_s/D value as the spacing changes however the fluctuations are smaller than those at the pier.

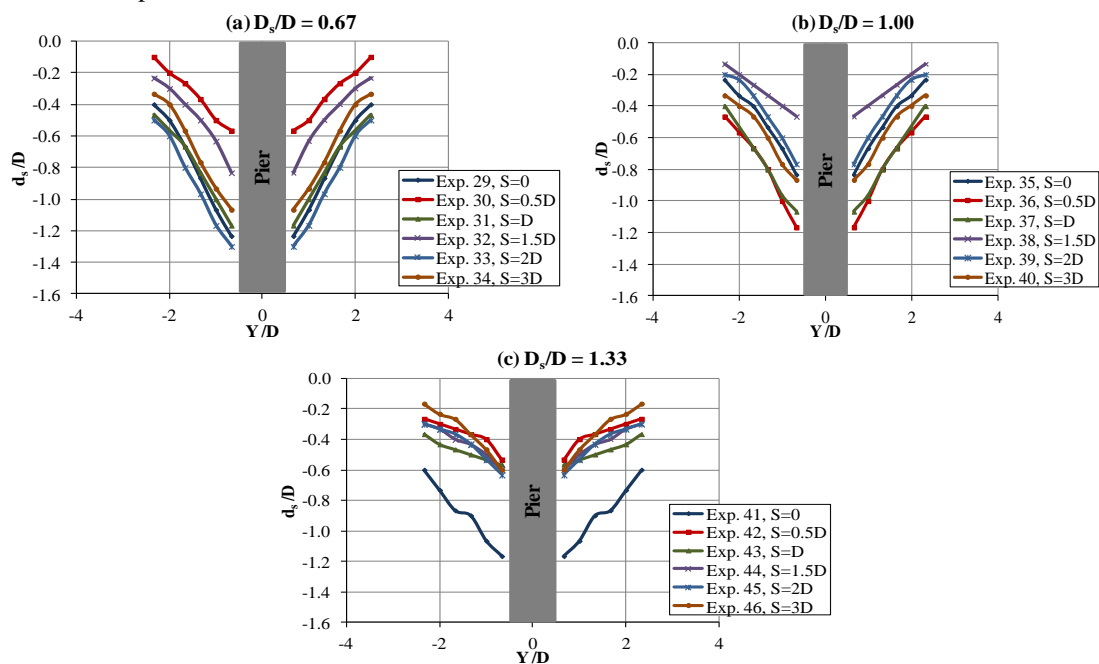


Fig. 11 Normalized scour hole profile in the transverse direction at the pier for $F_r=0.2$; (a) $D_s/D=0.67$, (b) $D_s/D=1.00$, and (c) $D_s/D=1.33$

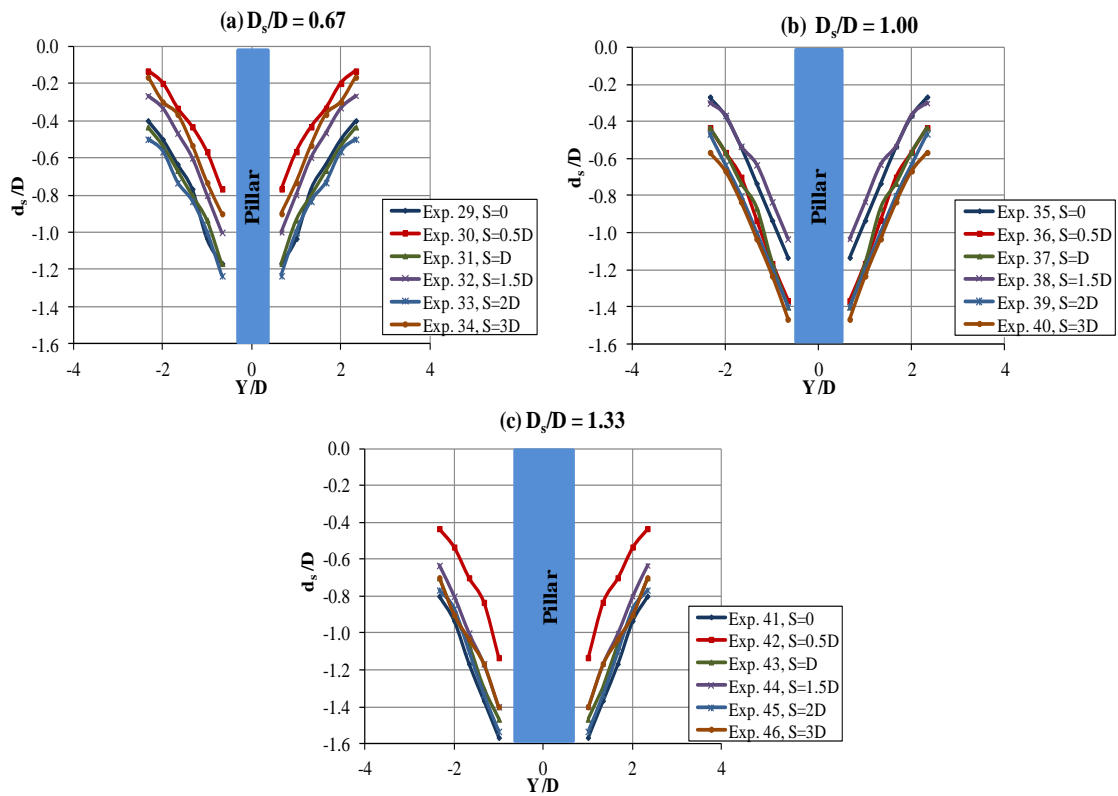


Fig. 12 Normalized scour hole profile in the transverse direction at the pillar for $F_r=0.2$; (a) $D_s/D=0.67$, (b) $D_s/D=1.00$, and (c) $D_s/D=1.33$

To assess the effect of the pillar in the different cases, a comparison of the scour depth at the pier between the case of the pier-alone at $F_r=0.2$ under clear water scour, i.e. experiment 20, and the different cases of the pier-pillar, i.e. experiments 29 to 46, has been made. This is performed by using the percentage reduction in the maximum depth of scour measured at the pier, %RMDS, where:

$$\%RMDS = \frac{d_{smo} - d_{sm}}{d_{smo}} \times 100 \tag{6}$$

Where d_{smo} is the maximum scour depth at the pier for the pier-alone case at $F_r=0.2$ under clear water scour, i.e. experiment 20 and d_{sm} is the maximum scour depth at the pier for the pier-pillar cases in experiments 29 to 46.

Fig. 13 shows the %RMDS, in the stream wise direction and in the transverse direction for different S/D and D_s/D cases. For the case of $S=0$, the scour depth at the pier, d_{sm} , in the stream wise direction is taken equal to that in the transverse direction at the centerline of the pier, otherwise d_{sm} is measured right upstream of the pier. The figure shows that there is a reduction in the maximum scour depth in the pier-pillar case compared to that of the pier-alone case in both the stream wise and the transverse direction. This demonstrates the effect of the pillar in reducing the local scour at the pier. The figure illustrates that the maximum reduction in the scour depth for $D_s/D=0.67$ and for $D_s/D= 1.33$ is reached at $S/D=0.5$, while for $D_s/D= 1.00$ the minimum scour depth is reached at $S/D=1.5$. The effectiveness of the pier-pillar technique is confirmed by assessing the reduction percentages in the scour depth in the stream wise X-direction at the pier, Fig. 12 (a), where the scour depth is reduced by 52% for the case of $S/D=0.5$ and $D_s/D=0.67$, by 54% for $S/D=0.5$ and $D_s/D=1.33$, and the maximum reduction of 57% is achieved for $S/D=1.5$ and $D_s/D=1.00$. Furthermore, the same conclusion can be drawn from Fig 12 (b), in the transverse direction, where the %RMDS is 62% for the case of $S/D=0.5$ and $D_s/D=0.67$, and is 64% for $S/D=0.5$ and $D_s/D=1.33$, and the greatest %RMDS of 69% is achieved for $S/D=1.5$ and $D_s/D=1.00$. From the practical point of view, constructing a pillar at 1.5D from the pier will be easier than constructing it at 0.5D. It is to be noted that such reduction percentages in the scour hole depth are notably higher than those reported by [16] using upstream triangular subsidiary pillar where they reported maximum reduction of approximately 28% that was obtained using S/D of 3 and α (the apex angle facing the approach flow) of 90° .

Fig. 13 presents the relationship between the diameters ratio D_s/D and the normalized spacing S/D . The cases with the maximum %RMDS in Fig. 12 were selected to construct Fig. 13 which can be used as a design curve for selecting the optimal spacing and pier pillar diameter ratio. The figure shows that as the diameter ratio

deviates from 1, the spacing should be smaller than that for $D_s/D=1$. For practical considerations, a spacing of $1.5D$ for $D_s/D=1$ may be considered the best.

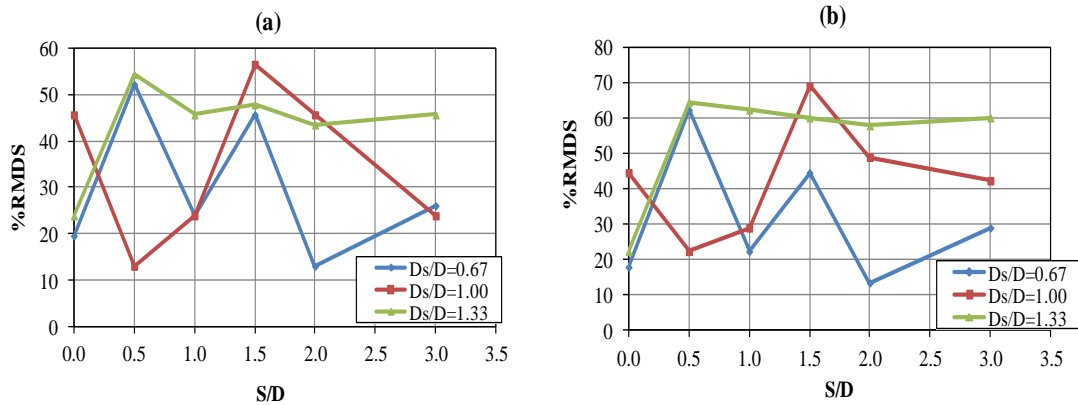


Fig. 13 Percentage reduction in the maximum depth of scour, RMDS, against spacing ratio, S/D, for different pillar diameter ratios, D_s/D ; (a) Streamwise direction. (b) Transverse Direction

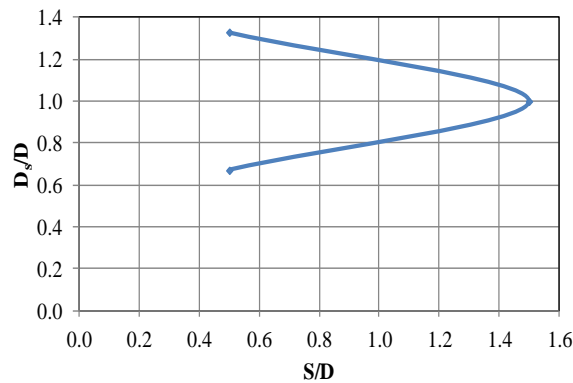


Fig. 14 Design curve for the optimal diameter and optimal spacing for the subsidiary pillar

V. Conclusions

This study presents the results obtained from an experimental investigation on using a circular subsidiary pillar, to be located upstream of the bridge pier, as a pier-scour countermeasure. The results showed that using the subsidiary pillar was very effective as a flow altering countermeasure that reduces the scour depth by more than 52% under clear water scour conditions in non-uniform sandy soil ($d_{50}=0.9\text{mm}$). Furthermore, the results reveal that the maximum reduction in the local scour depth was achieved when $D_s/D=1$ and $S=1.5D$ or when $D_s/D=2/3$ or $4/3$ and $S=0.5D$.

Acknowledgement

The authors would like to thank the Research Center at the College of Engineering of King Saud University for the provided technical and financial support that helped accomplishing this study. Thanks extend to Engineer Sami Alshehri for collecting the data for this study.

References

- [1]. E. V. Richardson and S. R. Davis, *Evaluating Scour at Bridges*, 4th Ed, Hydraulic Engineering Circular No 18, Report. No. FHWA NHI 01- 001, (Washington, D.C.:U.S. Dep of Transportation, Federal Highway Administration,2001).
- [2]. L. Briaud, K. Ting, C. Chen, R. Gudavalli, S. Perugu and G. Wei, Prediction of scour rate in cohesive soils at bridge piers, *J. Geotech. Geoenviron. Eng. ASCE*, vol.125, 1999, 237-246.
- [3]. M. Beg and S. Beg, Scour reduction around bridge piers: A review, *International Journal of Engineering Inventions*, 2 (7), 2013, 7-15.
- [4]. A. Jahangirzadeh, H. Bassar, S. Akib, S. Karami and S. Shamshirband, Experimental and numerical investigation of the effect of different shapes of collars on the reduction of scour around a single bridge pier, *PLoS ONE*, vol. 9, 2014, Article ID e98592.
- [5]. W. H. Graf and M. S. Altinakar, *Fluvial hydraulics: flow and transport processes in channels of simple geometry* (California: Wiley, 1998).
- [6]. B. W. Melville and S. E. Coleman, *Bridge scour* (Colorado: Water Resources Publication, 2000).
- [7]. L. Brandimarte, P. Paron and G. Di Baldassarre, Bridge pier scour: a review of processes, measurements and estimates, *Environmental Engineering & Management Journal*, 11 (5), 2012, pp. 975-989.
- [8]. A. J. Raudkivi, Scour at bridge piers, in *Scouring: hydraulic structures design manual*, (Florida: CRC Press, 1991) 61-98.
- [9]. H. W. Shen, V. R. Schneider, and S. Karaki, Local scour around bridge piers, *Journal of Hydraulic Division, ASCE*, 95(6), 1969, pp. 1919-1940.
- [10]. Y. M. Chiew, Failure mechanisms of riprap layer around bridge piers, in *First International Conference on Scour of Foundations*, Texas, 2002, 70-91.
- [11]. T. Hong-Wu, D. Bing, Y. M. Chiew and F. A. N. G. Shi-Long, Protection of bridge piers against scouring with tetrahedral frames, *International Journal of Sediment Research*, 24 (4), 2009, 385-399.
- [12]. M. A. Haque, M. M. Rahman, G. T. Islam and M. A. Hussain, Scour mitigation at bridge piers using sacrificial piles, *International Journal of Sediment Research*, 22(1), 2007, 49-59.
- [13]. Y. M. Chiew and Y. Y. Chen, Effect of suction on clear-water scour at bridge piers, *Fourth International Conference on Scour and Erosion*, Tokyo, Japan, 2008, 388-394.
- [14]. S. Soltani-Gerdefaramarzi, H. Afzalimehr, Y. M. Chiew and J. S. Lai, Jets to control scour around circular bridge piers, *Canadian Journal of Civil Engineering*, 40(3), 2013, 204-212.
- [15]. E. A. EL-Ghorab, Reduction of scour around bridge piers using a modified method for vortex reduction, *Alexandria Engineering Journal*, 52 (3), 2013, 467-478.
- [16]. H. Fouli and H. Elsebaie, Reducing local scour at bridge piers using an upstream subsidiary triangular pillar, *Arabian J. of Geosciences*,9(12), 2016, 598.
- [17]. S. Akib, N. Liana Mamat, H. Bassar and A. Jahangirzadeh, Reducing local scouring at bridge piles using collars and geobags, *The Scientific World Journal*, vol. 2014, 2014, 1-7.
- [18]. M. B. Mashahir, A. R. Zarrati, M. J. Rezaei and M. Zokaei, "Effect of collars and bars in reducing the local scour around cylindrical bridge piers, *International Journal of Engineering, Transaction B: Applications*, 22(4), 2009, 333-342.

HeshamFouli."Using A Subsidiary Pillar For Local Scour Mitigation At Bridge Piers."
IOSR Journal of Mechanical and Civil Engineering (IOSR-JMCE) , vol. 14, no. 6,
2017, pp. 38-49